

# 1 **Metabolic dissimilarity determines the establishment of cross-feeding** 2 **interactions in bacteria**

3  
4 Samir Giri<sup>1,2,\*</sup>, Leonardo Oña<sup>2</sup>, Silvio Waschina<sup>3,4</sup>, Shraddha Shitut<sup>1,2,#</sup>, Ghada  
5 Yousif<sup>1,2,5</sup>, Christoph Kaleta<sup>4</sup>, and Christian Kost<sup>1,2,\*</sup>

6  
7 <sup>1</sup> Experimental Ecology and Evolution Research Group, Department of Bioorganic  
8 Chemistry, Max Planck Institute for Chemical Ecology, 07745 Jena, Germany

9 <sup>2</sup> Department of Ecology, School of Biology/Chemistry, University of Osnabrück, 49076  
10 Osnabrück, Germany

11 <sup>3</sup> Institute for Human Nutrition and Food Science, Nutriinformatics, Christian-Albrechts-  
12 University Kiel, 24105 Kiel, Germany

13 <sup>4</sup> Research Group Medical Systems Biology, Institute for Experimental Medicine,  
14 Christian-Albrechts-University Kiel, 24105 Kiel, Germany

15 <sup>5</sup> Department of Botany and Microbiology, Faculty of Science, Beni-Suef University,  
16 Beni-Suef, Egypt

17  
18 \* Correspondence: christiankost@gmail.com (CKo), samirgiri2809@gmail.com (SG)

19  
20 # Current address: Institute of Biology, University of Leiden, 2333 Leiden, The  
21 Netherlands.

## 22 23 24 **Abstract**

25 The exchange of metabolites among different bacterial genotypes is key for  
26 determining the structure and function of microbial communities. However, the factors  
27 that govern the establishment of these cross-feeding interactions remain poorly  
28 understood. While kin selection theory predicts that individuals should direct benefits  
29 preferentially to close relatives, the potential benefits resulting from a metabolic  
30 exchange may be larger for more distantly related species. Here we distinguish  
31 between these two possibilities by performing pairwise cocultivation experiments  
32 between auxotrophic recipients and 25 species of potential amino acid donors.  
33 Auxotrophic recipients were able to grow in the vast majority of pairs tested (78%),  
34 suggesting that metabolic cross-feeding interactions are readily established. Strikingly,  
35 both the phylogenetic distance between donor and recipient as well as the dissimilarity  
36 of their metabolic networks was positively associated with the growth of auxotrophic  
37 recipients. Finally, this result was corroborated in an *in-silico* analysis of a co-growth  
38 of species from a gut microbial community. Together, these findings suggest metabolic  
39 cross-feeding interactions are more likely to establish between strains that are  
40 metabolically more dissimilar. Thus, our work identifies a new rule of microbial  
41 community assembly, which can help predict, understand, and manipulate natural and  
42 synthetic microbial systems.

43

## 44 **Keywords**

45 Bacterial community, community assembly, cross-feeding, metabolic distance,  
46 metabolite secretion, niche overlap, phylogenetic relatedness, public good.

47

## 48 **Significance**

49 Metabolic cross-feeding is critical for determining the structure and function of natural  
50 microbial communities. However, the rules that determine the establishment of these  
51 interactions remain poorly understood. Here we systematically analyze the propensity  
52 of different bacterial species to engage in unidirectional cross-feeding interactions. Our  
53 results reveal that synergistic growth was prevalent in the vast majority of cases  
54 analyzed. Moreover, both phylogenetic and metabolic dissimilarity between donors  
55 and recipients favored a successful establishment of metabolite exchange interactions.  
56 This work identifies a new rule of microbial community assembly that can help predict,  
57 understand, and manipulate microbial communities for diverse applications.

58

## 59 **Introduction**

60 Microorganisms are ubiquitous on our planet and are key for driving vital ecosystem  
61 processes (1-3). They contribute significantly to the flow of elements in global  
62 biogeochemical cycles (3, 4) and are also crucial for determining the fitness of plants  
63 (5, 6) and animals (7, 8) including humans (9, 10). These vital functions are provided  
64 by complex communities that frequently consist of hundreds or even thousands of  
65 metabolically diverse strains and species (11, 12). However, the rules that determine  
66 the assembly, function, and evolution of these microbial communities remain poorly  
67 understood. Yet understanding the underlying governing principles is central to  
68 microbial ecology and crucial for purposefully designing microbial consortia for  
69 biotechnological (13) or medical applications (14, 15).

70 In recent years, both empirical and theoretical work increasingly suggests that the  
71 exchange of essential metabolites among different bacterial genotypes is a key  
72 process that can significantly affect growth (16, 17), composition (18), and the structure  
73 of microbial communities (19). In those cases, one bacterial genotype releases a  
74 molecule into the extracellular environment, which can be used by other cells in the  
75 local vicinity. The released substances frequently include building block metabolites  
76 such as amino acids (20, 21), vitamins (22, 23), or nucleotides (24) as well as  
77 degradation products of complex polymers (19, 25). Even though these compounds  
78 represent valuable nutritional resources, they are released as unavoidable byproducts  
79 of bacterial physiology (26, 27) and metabolism (28) or due to leakage through the  
80 bacterial membrane (29, 30). Consequently, the released compounds create a pool of  
81 resources that can benefit both conspecifics and members of other species in the local  
82 neighborhood (31-34). The beneficiaries include genotypes that opportunistically take  
83 advantage of these metabolites as well as strains, whose survival essentially depends  
84 on an external supply with the corresponding metabolite. These so-called *auxotrophic*

85 genotypes carry a mutation in a biosynthetic or regulatory gene, which renders the  
86 resulting mutant unable to autonomously produce a certain metabolite such as an  
87 amino acid, a vitamin, or a nucleotide. By utilizing metabolites that are produced by  
88 another cell, a unidirectional cross-feeding interaction is generated. Auxotrophic  
89 mutants that use compounds released by others frequently gain a significant fitness  
90 advantage over prototrophic cells that produce the required metabolites by themselves  
91 (35). Due to the tremendous benefits that can result from this process, cross-feeding  
92 interactions are prevalent in all kinds of microbial ecosystems, including soil (36),  
93 fermented food (21), aquatic environments (37, 38), as well as host-associated  
94 microbiota (7, 39). Despite the ubiquity of unidirectional cross-feeding interactions in  
95 nature, the rules that govern their establishment remain poorly understood (40-43). In  
96 particular, it is unclear how the relationship between the metabolite donor and the  
97 auxotrophic recipient affects the likelihood that a cross-feeding interaction is  
98 successfully established. Two possibilities are conceivable.

99 First, kin selection theory predicts that organisms should preferentially direct  
100 benefits to close relatives rather than to more distantly related individuals (44). In this  
101 way, individuals indirectly favor the spread of their own genes. Even if the interaction  
102 at this stage is merely created by chance and has not evolved for this purpose, certain  
103 mechanisms might be in place that could maximize the chance that cells preferentially  
104 interact with conspecifics. Such mechanisms could be based, for example, on  
105 recognition alleles, as they play a role in other social interactions such as quorum  
106 sensing (45), biofilm formation (46), and swarming (47). Moreover, the exchange of  
107 metabolites could be mediated by contact-dependent interactions such as the  
108 formation of intercellular nanotubes (48, 49), which might require a close phylogenetic  
109 relatedness between donor and recipient for an efficient transport to operate. In the  
110 following, we refer to this possibility as the *similarity hypothesis*.

111 Second, unidirectional cross-feeding interactions might favor more distantly related  
112 donor-recipient pairs over interactions among close relatives. Two closely related  
113 bacterial cells are more likely to share ecological preferences such as habitat or  
114 resources utilized than two phylogenetically different bacterial taxa (41). Moreover, two  
115 genealogically related cells have greater similarities in their metabolic network than  
116 two distantly related cells (33, 50, 51). As a consequence, the biosynthetic cost to  
117 produce a given metabolite, and thus its nutritional value, is more likely to be different  
118 in heterospecific pairs than among members of the same species (52, 53). If these  
119 differences translate into enhanced growth of the auxotrophic recipient, a positive  
120 correlation between the growth of the auxotroph and the phylogenetic and/ or  
121 metabolic distance to the donor cell would be observed. In the following, we refer to  
122 this alternative possibility as the *dissimilarity hypothesis*.

123 Here we aim at distinguishing between these two hypotheses to better understand  
124 the rules that govern the establishment of this ecologically important interaction. To  
125 achieve this goal, we used unidirectional cross-feeding interactions as a model.  
126 Synthetically assembling pairs consisting of an auxotrophic recipient and a prototrophic  
127 amino acid donor of the same or a different species ensured that both interaction

128 partners do not share a common evolutionary history. In this way, all results will  
129 represent the situation of a naïve encounter between both interaction partners and only  
130 mirror effects resulting from the phylogenetic relatedness and metabolic dissimilarity  
131 between partners. Using this ecological approach, we systematically determined  
132 whether and how the phylogenetic or metabolic distance between auxotrophic  
133 recipients and prototrophic amino acid donors affects cross-feeding in pairwise  
134 bacterial consortia.

135 Our results show that in the vast majority of cases, unidirectional cross-feeding  
136 interactions successfully established between a prototrophic donor and an auxotrophic  
137 recipient. Strikingly, recipients' growth was positively associated with both, the  
138 phylogenetic and metabolic distance between donor and recipient. This pattern could  
139 partly be explained by the difference in the amino acid profiles produced by donors.  
140 Finally, an *in-silico* analysis of co-growth of species from a gut microbial community  
141 revealed that recipient genotypes benefitted more when interacting with metabolically  
142 dissimilar partners, thus corroborating the empirical results. Our work identifies the  
143 metabolic dissimilarity between donor and recipient genotypes as a key parameter for  
144 the establishment of unidirectional cross-feeding interactions.

145

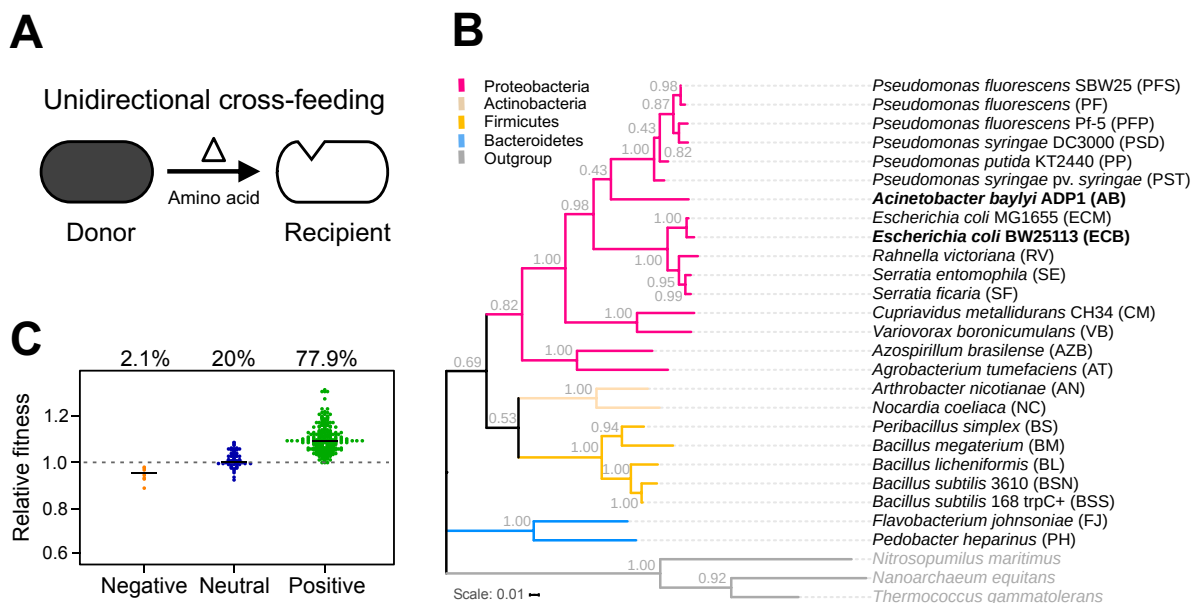
## 146 **Results**

147

### 148 **Auxotrophic recipients commonly benefit from the presence of prototrophic** 149 **donor cells**

150 To determine the probability, with which unidirectional cross-feeding interactions  
151 emerge between an auxotrophic recipient and a prototrophic donor genotype, a series  
152 of pairwise coculture experiments were performed (Fig. 1A). For this, 25 strains that  
153 belonged to 21 different bacterial species were used as potential amino acid donors  
154 (Figs. 1B and S1A). Donor strains were selected to cover both the existing diversity of  
155 bacterial taxa and the phylogenetic neighborhood of the focal auxotrophs as good as  
156 possible. These potential amino acid donors were individually cocultured together with  
157 one auxotrophic recipient of *Escherichia coli* or *Acinetobacter baylyi*, which were both  
158 auxotrophic for either histidine ( $\Delta hisD$ ) or tryptophan ( $\Delta trpB$ ) (Fig. S1B).

159 To test if the selected donor strains can support the growth of auxotrophic recipients,  
160 the abovementioned strains were systematically cocultured in all possible pairwise  
161 combinations (initial ratio: 1:1). Subsequently, the net growth of the recipient strains in  
162 coculture was quantified over 24 h, and compared to the growth, the same strain  
163 achieved in monoculture over the same period in the absence of amino acid. In this  
164 experiment, the donor's presence affected the recipient's growth either positively,  
165 negatively, or in a neutral way. Only 2% of the tested cases showed a growth reduction,  
166 and in 20% of the interactions, auxotrophs did not respond at all to the presence of a  
167 donor cell (Fig. 1C). In contrast, in the vast majority of cocultures tested (i.e., 78%),  
168 auxotrophic cells grew significantly better in the presence of donor cells than  
169 monocultures of auxotrophs, suggesting that unidirectional cross-feeding interactions  
170 can readily establish (Fig. 1C).



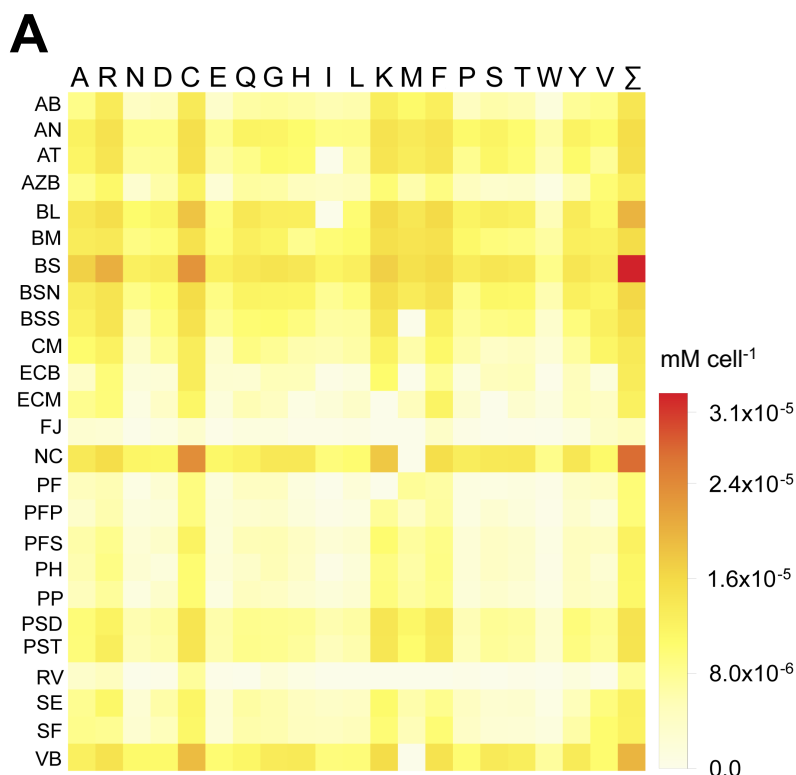
171

172 **Fig. 1. Unidirectional cross-feeding between prototrophic donor cells and amino acid**  
 173 **auxotrophic recipients is common. (A)** Overview over the experimental system used.  
 174 Metabolically autonomous donor genotypes (dark cell) were cocultivated together with an  
 175 auxotrophic recipient that was unable to produce either histidine or tryptophan (white cell).  
 176 Growth of auxotrophs signifies the successful establishment of a unidirectional cross-feeding  
 177 interaction, in which the focal amino acid ( $\Delta$ ) is exchanged between both cells. **(B)**  
 178 Phylogenetic tree of bacterial species (donors and recipients) used in this study. Different  
 179 colors indicate different phyla. The tree was constructed based on the 16S rRNA gene.  
 180 Recipient strains used in this study are highlighted in bold. Branch node numbers represent  
 181 bootstrap support values. **(C)** Growth of auxotrophic recipients in pairwise coculture with  
 182 different donor genotypes. *Escherichia coli* and *Acinetobacter baylyi*, each either auxotrophic  
 183 for histidine ( $\Delta hisD$ ) or tryptophan ( $\Delta trpB$ ), were used as amino acid recipients. The relative  
 184 fitness of receivers when grown in coculture with one of X donors is plotted relative to their  
 185 growth in monoculture in the absence of the focal amino acid (dashed line). CFU was  
 186 calculated 24 h post-inoculation. Interactions in cocultures were classified as negative (n = 8),  
 187 neutral (n = 76), and positive (n = 296), based on the statistical difference between the growth  
 188 of auxotrophs in monoculture and coculture (FDR-corrected paired t-test:  $P \leq 0.05$ , n = 4).

189

## 190 Recipient growth depends on amino acid production of donor genotypes

191 The main factor causing the growth of auxotrophs in the coculture experiments  
 192 was likely the amount and identity of metabolites that donor cells released into the  
 193 extracellular environment (i.e., the exo-metabolome) (26). To test if amino acid  
 194 production of donors could explain the observed recipient growth, the supernatant of  
 195 monocultures of all 25 donor strains was collected during exponential growth.  
 196 Subjecting the cell-free supernatant of these cultures to LC/MS/MS analysis revealed  
 197 that all tested genotypes secreted amino acids in varying amounts (Figs. 2A and S2).  
 198



**B**

Supernatant experiment

Total amino acids			
Recipient	n	$\rho$	P-value
AB-his	89	0.29	<b>4.3x10<sup>-3</sup></b>
AB-trp	90	0.17	0.12
ECB-his	92	0.35	<b>8.3x10<sup>-4</sup></b>
ECB-trp	93	0.33	<b>1.2x10<sup>-3</sup></b>
Focal amino acid			
Recipient	n	$\rho$	P-value
AB-his	89	0.23	<b>0.029</b>
AB-trp	90	0.09	0.37
ECB-his	92	0.47	<b>0.2x10<sup>-5</sup></b>
ECB-trp	93	0.43	<b>0.13x10<sup>-4</sup></b>

199

200 **Fig. 2. Total amino acids production of different donors can predict unidirectional cross-**  
 201 **feeding. (A)** Heatmap of amino acids released by different donor strains. Amount of amino  
 202 acid (mM per cell) produced by 25 donor strains (for abbreviations see Fig. 1B) is shown (Y-  
 203 axis). Cell-free supernatants of exponentially growing cultures were analyzed via LC/MS/MS.  
 204 Colors indicate different amino acid concentrations (legend).  $\Sigma$  = total amino acid produced by  
 205 the donor. **(B)** Overview over the statistical relationships between the total amount of amino  
 206 acids (upper part) or the focal amino acid (lower part) in supernatants of donor cultures and  
 207 the growth of the corresponding auxotrophic recipients. Results of spearman rank correlations  
 208 ( $\rho$ ) are shown.

209

210 In this experiment, donors are not expected to specifically produce the amino acid that  
 211 the cocultured auxotroph requires for growth. Moreover, bacteria usually use generic

212 transporters that transport similar types of amino acids across the membrane (54-56).  
213 Thus, auxotrophic recipients may benefit not only from the one amino acid they require  
214 for growth, but also from utilizing the other amino acids that are produced by the donor.  
215 To quantitatively determine whether the released amino acids could explain the growth  
216 of recipient cells, the conditioned cell-free supernatant was supplied to monocultures  
217 of auxotrophic cells and the resulting growth over 24 h was quantified. In addition, the  
218 chemical composition of the supernatants used was determined via LC/MS/MS. This  
219 experiment revealed that donor supernatants enhanced the growth of auxotrophic  
220 recipients. Interestingly, recipient growth correlated positively with the total amount of  
221 amino acids that were present in the supernatant (Table 2B). In addition, growth of  
222 auxotrophic recipients was positively associated with the concentration of the amino  
223 acid auxotrophs required for growth as well as with the total amount of amino acids  
224 produced by donor cells (Table 2B). Together, these results show that auxotrophic  
225 recipients not only use the amino acids they cannot produce on their own, but also take  
226 advantage of the other amino acids that are produced by donor cells.

227

### 228 **Recipient growth correlates positively with amino acid profile dissimilarity**

229 To distinguish between the two main hypotheses, we asked whether the difference  
230 in the amino acid profile produced by a closely and distantly related donor strain could  
231 explain the growth auxotrophs achieved in the coculture experiment. To test this, we  
232 calculated the Euclidean distance between the amino acid profiles of all 25 donor  
233 strains. Assessing the statistical relationship between the normalized growth of  
234 auxotrophs in coculture with the Euclidean distance in the amino acid profiles of closely  
235 and distantly related donor genotypes revealed a significant positive relationship  
236 between both parameters in all cases (Fig. 3A and Table 1). In other words, auxotrophs  
237 grew better in coculture with a donor, which contained an amino acid mixture that was  
238 different from the one a conspecific cell would have produced. Thus, these results  
239 provide evidence that supports the dissimilarity hypothesis.

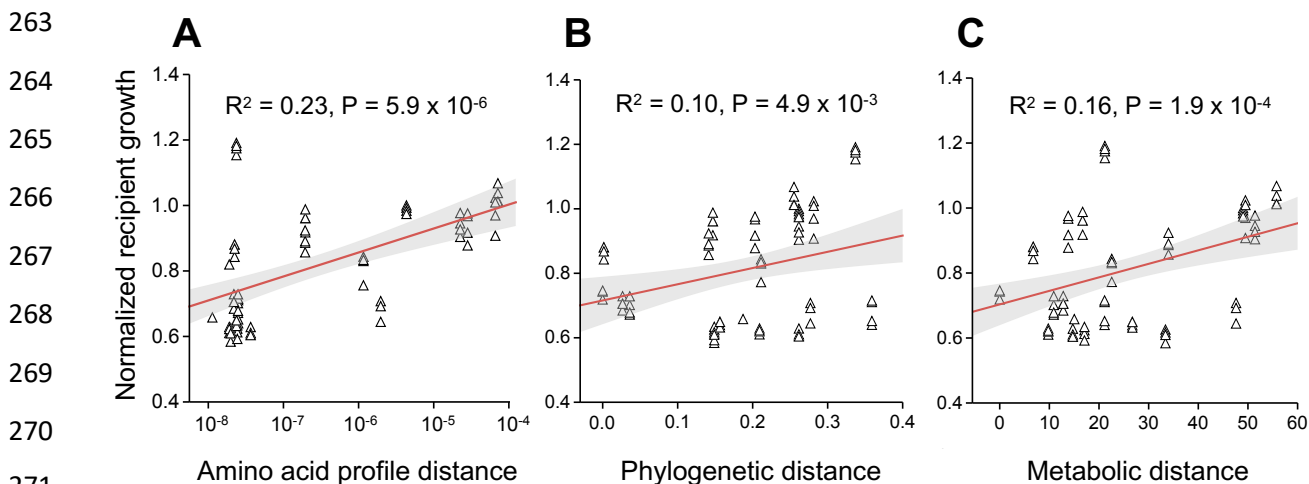
240

### 241 **Growth of recipients scales positively with the phylogenetic and metabolic 242 distance to donor cells**

243 Next, we asked whether two phylogenetically close genotypes are more likely to  
244 engage in a unidirectional cross-feeding interaction than two more distantly related  
245 genotypes. To test this, we re-analyzed the results of the coculture experiment by  
246 focusing on the phylogenetic relatedness between donor and recipient genotypes. In  
247 this context, only those cocultures were considered, in which auxotrophs showed  
248 detectable growth. These analyses revealed a positive association between the growth  
249 of recipients and the phylogenetic distance to donor cells (Fig. 3B and Table 1).

250 However, given that previous analyses suggested that differences in the amino acid  
251 profiles could predict auxotrophic recipients' growth (Fig. 3A and Table 1), we  
252 hypothesized that the phylogenetic distance might only be a proxy for the difference in  
253 the strains' metabolic networks. To verify this hypothesis, we compared genome-scale  
254 metabolic networks of all donor and recipient genotypes. Using this data, a metabolic  
255 similarity matrix between donor and recipient strains was calculated by identifying

256 commonalities and differences in both partners' biosynthetic pathways. Correlating the  
 257 resulting data with the growth of auxotrophic recipients in coculture revealed again a  
 258 positive association between the metabolic distance and recipient growth (Fig. 3C and  
 259 Table 1). Together, these results provide additional support for the interpretation that  
 260 cross-feeding interactions are more likely to establish between two more dissimilar  
 261 genotypes.



272 **Fig. 3. Cross-feeding increases with an increasing dissimilarity to donor cells.** Shown is  
 273 the net growth of the *E. coli* recipient auxotrophic for histidine ( $\Delta hisD$ ,  $\triangle$ ) as a function of (A)  
 274 the amino acid profile distance, (B) the phylogenetic distance, and (C) the genome-based  
 275 metabolic distance between donor and recipient. Red lines are fitted linear regressions and  
 276 grey area indicates the 95% confidence interval. Sample size is 80 in all cases. Growth of  
 277 recipient is displayed as a logarithm of the difference in number of CFUs between 0 h and 24  
 278 h and was normalized per number of donor cells.

279  
 280 **Table 1. Amino acid profile distance (AAD), phylogenetic distance (PD), and metabolic**  
 281 **distance (MD), is positively associated with recipient growth.** Results of statistical  
 282 regressions are shown.

Recipient	n	R <sup>2</sup>	AAD P-value	R <sup>2</sup>	PD P-value	R <sup>2</sup>	MD P-value
AB-his	87	0.16	<b>8.0x10<sup>-5</sup></b>	0.45	<b>1.61x10<sup>-12</sup></b>	0.26	<b>3.82x10<sup>-7</sup></b>
AB-trp	100	0.07	<b>5.5x10<sup>-3</sup></b>	0.11	<b>7.92x10<sup>-4</sup></b>	0.19	<b>5.59x10<sup>-6</sup></b>
ECB-his	80	0.23	<b>5.9x10<sup>-6</sup></b>	0.10	<b>4.95x10<sup>-3</sup></b>	0.16	<b>1.96x10<sup>-4</sup></b>
ECB-trp	91	0.26	<b>2.1x10<sup>-7</sup></b>	0.12	<b>6.40x10<sup>-4</sup></b>	0.17	<b>3.80x10<sup>-5</sup></b>

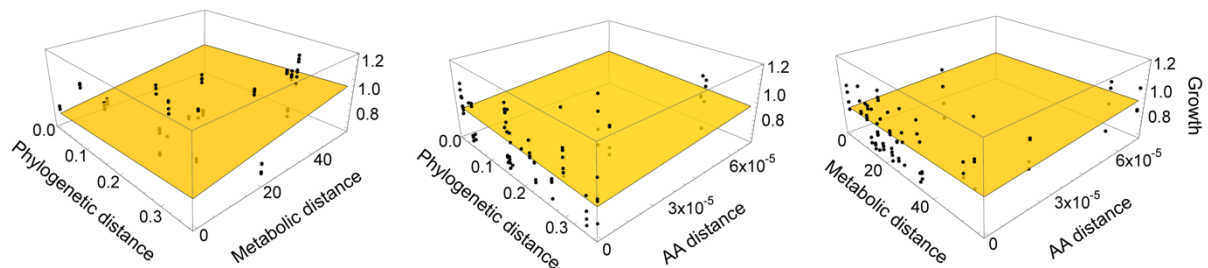
283  
 284  
 285 **All three distance measures alone can explain recipient growth**  
 286 Having observed a significant positive correlation of recipient growth with each of  
 287 the three-distance metrics analyzed (i.e., amino acid profile distance (AAD),  
 288 phylogenetic distance (PD), and metabolic distance (MD), Table 1), we asked whether  
 289 these factors alone were sufficient to predict the growth of auxotrophic recipients. This  
 290 question was addressed by replotting the data of the performed coculture experiments  
 291 in three-dimensional graphs that display the growth of a given auxotroph depending



292 on two of the three measures quantified. Fitting a 2D plane into the resulting graphs  
293 indicated that increasing each of the three measures also increased recipients' growth  
294 (Fig. 4 and S3). Thus, these graphs suggested that the three explanatory variables are  
295 likely correlating with each other. To subject this conjecture to a formal statistical test,  
296 we repeated the regression analyses to examine whether MD or AAD were significantly  
297 associated with the growth of auxotrophs in coculture, when the first predictor variable  
298 PD was already included (Table S1). In all cases, growth of *E. coli* recipients remained  
299 positively associated with metabolic distance as well as the distance of the amino acid  
300 production profile (Table S1). However, this pattern no longer holds for *A. baylyi*  
301 auxotrophs ( $\Delta hisD$  and  $\Delta trpB$ ) (Table S1).

302 Furthermore, we hypothesize that the amount of amino acid produced by the donors  
303 should affect recipient growth. Genotypically related donors are more likely to produce  
304 the same spectrum of amino acids as compared to distantly related individuals. In order  
305 to consider this fact, we performed additional analyses that controlled for the role of  
306 total amino acid production or focal amino acid production (his or trp). In almost all  
307 cases, growth of recipients remained significantly positively associated with the three  
308 distance measures (Table S2 and S3). Together, the set of analyses performed  
309 demonstrates that the three different measures analyzed (i.e., AAD, PD, and MD, and)  
310 can individually (in the case of *E. coli*) or in combination (both species) explain the  
311 cross-feeding between prototrophic donors and auxotrophic recipients, thus,  
312 corroborating the dissimilarity hypothesis.

313



314

315 **Fig. 4. Multiple distance measures interactively explain recipient growth.** The plane  
316 depicts the linear regression between the growth of the histidine auxotrophic *E. coli* recipient  
317 ( $\Delta hisD$ ) and the phylogenetic distance, the metabolic distance, and the amino acid profile  
318 distance between donor and recipient. Data points above the plane are shown in black. See  
319 also Fig. S3 for other comparisons.

320

### 321 ***In-silico* models predict that metabolic dissimilarity between species enhances** 322 **cross-feeding**

323 To verify whether the patterns we observed in laboratory-based coculture  
324 experiments also apply to natural microbial communities, we used *in-silico* modeling  
325 to simulate the co-growth of different bacterial species that co-occur in the human  
326 gastrointestinal tract. Specifically, we considered all of 334,153 pairwise combinations  
327 of 818 bacteria commonly found in this environment. The *in-silico* simulations indicated  
328 that the relationship between metabolic distance and metabolic exchange (i.e., total  
329 metabolic fluxes between species) follows a saturation curve (Fig. 5). In fact, fitting a  
330 logistic function resulted in a higher goodness of fit ( $P < 0.001$ ,  $R^2 = 0.04$ ) than fitting

331 a linear function ( $R^2 = 0.023$ ). This finding suggests that also bacteria residing within  
332 the human gut are more likely to engage in cross-feeding interactions with  
333 metabolically more dissimilar species. Taken together, the set of computational  
334 analyses performed here is in line with the experimental data shown above: both  
335 datasets reveal that metabolic cross-feeding interactions are more likely to establish  
336 between two metabolically more dissimilar partners.

337

338

339

340

341

342

343

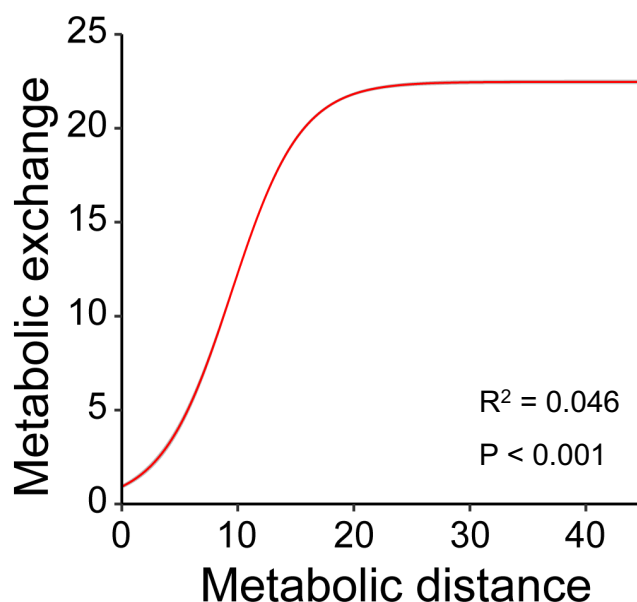
344

345

346

347

348



349 **Fig. 5. Metabolic exchange increases with an increasing metabolic distance between**  
350 **interaction partners in gut microbial communities.** Shown is the result of an *in-silico* flux-  
351 balance-analysis of paired models analyzing 334,153 combinations of 818 bacterial species  
352 residing in the human gut. Results of a logistic model (red line) and the 95% confidence interval  
353 (grey area) are displayed.

354

## 355 Discussion

356 Metabolic cross-feeding interactions among different microbial species are  
357 ubiquitous and play key roles in determining the structure and function of microbial  
358 communities (16, 57, 58). However, the rules that govern their establishment remain  
359 poorly understood. Here we identify the metabolic dissimilarity between donor and  
360 recipient genotype as a major determinant for the establishment of obligate,  
361 unidirectional cross-feeding interactions between two bacterial strains. In systematic  
362 coculture experiments between a prototrophic amino acid donor and an auxotrophic  
363 amino acid recipient, we show that growth of auxotrophic recipients in coculture was  
364 positively associated with (i) the compositional difference in the amino acid mixtures  
365 various donor produced (Fig. 3A), (ii) their phylogenetic distance (Fig. 3B), as well as  
366 (iii) the difference in their metabolic networks (i.e. their metabolic distance) (Fig. 3C).  
367 Furthermore, *in-silico* simulations of the co-growth of species from a gut microbial  
368 community corroborated that the propensity of cross-feeding interactions to establish  
369 increased when both interacting partners were metabolically more dissimilar (Fig 5).

370 In our study, we manipulated the relatedness between donor and recipient  
371 genotypes. A high phylogenetic relatedness between two genotypes (donor and  
372 recipient) in coculture means that they can perform similar metabolic reactions and are  
373 more likely to be characterized by overlapping growth requirements (33, 43). As a  
374 consequence, both the nutritional value of a given molecule and the biosynthetic cost  
375 to produce it is alike (52, 53, 59). In contrast, two phylogenetically distant strains likely  
376 differ in their metabolic capabilities and requirements. Thus, two more closely related  
377 strains are likely to compete for environmentally available nutrients and provide an  
378 increased potential for a difference in the cost-to-benefit-ratio than two distant relatives  
379 (43, 60). This statistical relationship can explain why in our coculture experiments, both  
380 the phylogenetic and metabolic distance was positively associated with the growth of  
381 cocultured auxotrophs. Thus, our results support the dissimilarity hypothesis to explain  
382 the establishment of unidirectional cross-feeding interactions. Our findings are in line  
383 with previous studies that analyzed the effect of the phylogenetic relatedness and  
384 metabolic dissimilarity on antagonistic interactions between two different genotypes.  
385 The authors of these studies found that bacteria mainly inhibit the growth of  
386 metabolically more similar and related species (41, 61). Even though the focal  
387 biological process differs drastically between our (metabolic cross-feeding) and these  
388 other studies (antagonistic interactions), the main finding is conceptually equivalent:  
389 genotypes are more likely to compete against close relatives, yet support the growth  
390 of more dissimilar strains – either by enhancing their growth (Fig. 3) or inhibiting them  
391 less (41, 61).

392 In our experiments, we took advantage of synthetically assembled pairwise  
393 interactions between different bacterial genotypes to assess how the similarity  
394 between interacting partners affects the cross-feeding of metabolites. Even though this  
395 approach is limited by the number of pairwise comparisons that can be analyzed in  
396 one experiment, the obtained results provide a very clear answer to the focal question.  
397 First, the selected donor strains covered a broad range of taxonomic diversity in  
398 bacteria (Fig. 1B). Thus, the spectrum of ecological interactions analyzed here likely  
399 reflects the range of interactions a given bacterial genotype would typically experience  
400 in a natural microbial community. Second, by deliberately choosing strains that lack a  
401 previous coevolutionary history, any result observed can be clearly attributed to the  
402 focal, experimentally-controlled parameter (e.g., phylogenetic or metabolic distance).  
403 In this way, confounding effects like an evolved preference for a certain genotype can  
404 be ruled out. Finally, we analyzed bacterial consortia in a well-mixed, spatially  
405 unstructured environment, in which the exchanged metabolites are transferred  
406 between cells via diffusion through the extracellular environment. Such a set-up  
407 minimizes factors that would be amplified in a spatially structured environment, such  
408 as a local competition for nutrients or the release of metabolic waste products that  
409 inhibit the growth of other cells in the local vicinity. Thus, the experimental approach  
410 chosen circumvents the challenges of manipulating and detecting metabolite  
411 exchange in natural environments and instead capitalizes on analyzing experimentally  
412 arranged and carefully controlled coculture experiments.

413 The guiding principle discovered in this study is most likely relevant for ecological  
414 interactions outside the realm of microbial communities. Mutualistic interactions, in  
415 which two partners reciprocally exchange essential metabolites or services, usually  
416 involve two or more completely unrelated species (60, 62-64). In contrast, cooperative  
417 interactions among closely related individuals usually rely on the uni- or bidirectional  
418 exchange of the same commodity or service (60). Thus, the fact that two more  
419 dissimilar individuals have an increased potential to engage in a synergistic interaction  
420 than two more similar individuals may be a universal rule that guides the establishment  
421 of mutualistic interactions in general (43).

422 Our results highlight the utility of using synthetic, laboratory-based model systems  
423 to understand fundamental principles of microbial ecology. In this study, we  
424 demonstrated that the establishment of interactions in complex natural communities is  
425 likely determined by simple rules of assembly. These insights not only enrich our  
426 understanding of complex microbial communities, but also help us to engineer them  
427 for biotechnological or medical applications.

428

## 429 **Material and methods**

430

### 431 *Bacterial strains and their construction*

432 Twenty-five bacterial wild type strains were used as potential amino acid donors  
433 (Supplemental Table S4). *Escherichia coli* BW25113 and *Acinetobacter baylyi* ADP1  
434 were used as parental strains, from which mutants that are auxotrophic for histidine  
435 ( $\Delta hisD$ ) or tryptophan ( $\Delta trpB$ ) were generated. The gene to be deleted in order to  
436 create the corresponding auxotrophy was identified using the KEGG (65) and the  
437 EcoCyc (66) database. For *E. coli*, deletion alleles were transferred from existing single  
438 gene deletion mutants (i.e. the Keio collection, (67)) into *E. coli* BW25113 using phage  
439 P1-mediated transduction (68). In-frame knockout mutants were achieved by the  
440 replacement of target genes with a kanamycin resistance cassette. In the case of *A.*  
441 *baylyi*, deletion mutants were constructed as described previously (48). Briefly, linear  
442 constructs of the kanamycin resistance cassette with 5'-overhangs homologous to the  
443 insertion site were amplified by PCR, where pKD4 was used as a template (see  
444 Supplemental Table S5 for primer details). Upstream and downstream regions  
445 homologous to *hisD* and *trpB* were amplified using primers with a 5'-extension that was  
446 complementary to the primers used to amplify the kanamycin resistance cassette. The  
447 three amplified products (upstream, downstream, and kanamycin) were combined by  
448 PCR, resulting in overhanging flanks with a kanamycin cassette. This PCR product  
449 was introduced into the *A. baylyi* WT strain. For this, the natural competence of *A.*  
450 *baylyi* was harnessed. Transformation was done by diluting 20  $\mu$ l of a 16 h-grown  
451 culture in 1 ml lysogeny broth (LB). This diluted culture was mixed with 50  $\mu$ l of the  
452 above PCR mix and further incubated at 30 °C with shaking at 200 rpm for 3 h. Lastly,  
453 1 ml volume was pelleted, washed once with LB broth, plated on LB agar plates  
454 containing kanamycin (50  $\mu$ g ml<sup>-1</sup>), and incubated at 30 °C for colonies to grow.

455 Conditional lethality of constructed auxotrophic mutations in MMAB medium was  
456 verified by inoculating  $10^5$  colony-forming units (CFU)  $\text{ml}^{-1}$  of these strains into 1 ml  
457 MMAB medium with or without the focal amino acid ( $100 \mu\text{M}$ ). After 24 h, their optical  
458 density (OD) was determined spectrophotometrically at 600 nm using FilterMax F5  
459 multi-mode microplate reader (Molecular Devices) and the mutation was considered  
460 conditionally essential when growth did not exceed the  $\text{OD}_{600\text{nm}}$  of uninoculated  
461 minimal medium (67, 69).

462

#### 463 *Culture conditions and general procedures*

464 A modified minimal media for *Azospirillum brasilense* (MMAB, (70)) was used for all  
465 experiments containing  $\text{K}_2\text{HPO}_4$  ( $3 \text{ g L}^{-1}$ ),  $\text{NaH}_2\text{PO}_4$  ( $1 \text{ g L}^{-1}$ ),  $\text{KCl}$  ( $0.15 \text{ g L}^{-1}$ ),  $\text{NH}_4\text{Cl}$   
466 ( $1 \text{ g L}^{-1}$ ),  $\text{MgSO}_4 \cdot 7\text{H}_2\text{O}$  ( $0.3 \text{ g L}^{-1}$ ),  $\text{CaCl}_2 \cdot 2\text{H}_2\text{O}$  ( $0.01 \text{ g L}^{-1}$ ),  $\text{FeSO}_4 \cdot 7\text{H}_2\text{O}$  ( $0.0025$   
467  $\text{g L}^{-1}$ ),  $\text{Na}_2\text{MoO}_4 \cdot 2\text{H}_2\text{O}$  ( $0.05 \text{ g L}^{-1}$ ), and  $5 \text{ g L}^{-1}$  D-glucose as a carbon source. 10 ml  
468 of trace salt solution was added per liter of MMAB media from the 1L stock. Trace salt  
469 stock solution consisted of filter sterilized  $84 \text{ mg L}^{-1}$  of  $\text{ZnSO}_4 \cdot 7\text{H}_2\text{O}$ ,  $765 \mu\text{l}$  from 0.1  
470 M stock of  $\text{CuCl}_2 \cdot 2\text{H}_2\text{O}$ ,  $8.1 \mu\text{l}$  from 1 M stock of  $\text{MnCl}_2$ ,  $210 \mu\text{l}$  from 0.2 M stock of  
471  $\text{CoCl}_2 \cdot 6\text{H}_2\text{O}$ ,  $1.6 \text{ ml}$  from 0.1 M stock of  $\text{H}_3\text{BO}_3$ ,  $1 \text{ ml}$  from  $15 \text{ g L}^{-1}$  stock of  $\text{NiCl}_2$ .

472 All strains were precultured in replicates by picking single colonies from LB agar  
473 plates, transferring them into 1 ml of liquid MMAB in 96-deep well plate (Eppendorf,  
474 Germany), and incubating these cultures for 20 h. In all experiments, auxotrophs were  
475 precultured at  $30^\circ\text{C}$  in MMAB, which was supplemented with  $100 \mu\text{M}$  of the required  
476 amino acid. The next day, precultures were diluted to an optical density of 0.1 at 600  
477 nm as determined by FilterMax F5 multi-mode microplate readers (Molecular Devices).

478

#### 479 *Coculture experiment*

480 Approximately  $50 \mu\text{l}$  of preculture were inoculated into 1 ml MMAB, leading to a  
481 starting density 0.005 OD. In case of cocultures, donor and recipient were mixed in a  
482 1:1 ratio by co-inoculating  $25 \mu\text{l}$  of each diluted preculture without amino acid  
483 supplementation. Monocultures of both donors and recipient (with and without the focal  
484 amino acid) were inoculated using  $50 \mu\text{l}$  of preculture. Cultures were incubated at a  
485 temperature of  $30^\circ\text{C}$  and shaken at 220 rpm. Cell numbers were determined at 0 h  
486 and 24 h by serial dilution and plating. Donor strains were plated on MMAB agar plates,  
487 whereas recipients (auxotrophs) were differentiated on LB agar containing kanamycin  
488 ( $50 \mu\text{g ml}^{-1}$ ) to select for recipient strains. For key resources, see (Supplemental Table  
489 S6).

490

#### 491 *Relative fitness measurement*

492 To quantify the effect of amino acid cross-feeding on the fitness of the recipient, the  
493 number of colony-forming units (CFU) per ml was calculated for monoculture and  
494 coculture conditions at 0 h and 24 h. Each donor was individually paired with one of  
495 the recipients as well as grown in monoculture. Every combination was replicated four  
496 times. The relative fitness of each recipient was determined by dividing the growth of  
497 each genotype achieved in coculture by the value of its respective monoculture. Since  
498 different donor genotypes show inherent differences in growth, the growth of recipients  
499 in coculture was normalized to reduce to minimize potential effects of this variation.

500 For this, growth of recipients in monoculture was first subtracted from its growth in  
501 coculture and then divided by the growth the respective donor genotype achieved in  
502 coculture.

503

#### 504 *Amino acid supernatant experiment*

505 To determine whether cross-feeding was mediated via compounds that have been  
506 released into the extracellular environment, the cell-free supernatants of donor  
507 genotypes were harvested and provided to receiver strains. To collect the supernatant,  
508 donors were grown in 2.5 ml MMAB in 48-deep well plates (Axygen, USA) and  
509 cultivated at 30 °C under shaking conditions (220 rpm). Supernatants were isolated in  
510 the mid-exponential growth phase and centrifuged for 10 min at 4,000 rpm. Then,  
511 supernatants were filter-sterilized (0.22 µm membrane filter, Pall Acroprep, USA) and  
512 stored at -20 °C. Meanwhile, receivers were grown in 1 ml MMAB in 96-well plates for  
513 24 h. After adjusting the receiver OD<sub>600nm</sub> to 0.1, 5 µl of the receiver culture was added  
514 to the replenished donor supernatant (total culturing volume: 200 µl, i.e. 160 µl donor  
515 supernatant + 40 µl MMAB) in 384-well plates (Greiner bio-one, Austria) (total: 50 µl  
516 culture). Four replicates of each comparison were grown for 24 h at 30 °C in a FilterMax  
517 F5 multi-mode microplate reader (Molecular Devices). MMAB without supernatant and  
518 monocultures of receiver strains were used as control. Growth was determined by  
519 measuring the optical density at 600 nm every 30 minutes, with 12 minutes of orbital  
520 shaking between measurements. OD<sub>600nm</sub> was measured and analyzed to calculate  
521 the maximum optical density (OD<sub>max</sub>) achieved by the receiver strain using the Softmax  
522 Pro 6 software (Table S7). For each donor supernatant-receiver pair, OD<sub>max</sub> achieved  
523 by receivers with supernatant was subtracted from the values achieved by cultures  
524 grown without supernatant and normalized with the OD<sub>600nm</sub>, the respective donor  
525 strain had achieved at the time of supernatant extraction.

526

#### 527 *Amino acid quantification by LC/MS/MS*

528 All 20 proteinogenic amino acids in the culture supernatant were analyzed. 100 µl  
529 of extracted supernatant was derivatized using the dansyl chloride method (71, 72).  
530 Norleucine was added as an internal standard to the sample and a calibration curve  
531 was generated by analyzing all 20 amino acids at different concentrations. All samples  
532 were directly analyzed via LC/MS/MS. Chromatography was performed on a Shimadzu  
533 HPLC system. Separation was achieved on an Accucore RP-MS 150 x 2.1, 2.6 µm  
534 column (Thermo Scientific, Germany). Formic acid 0.1% in 100% water and 80%  
535 acetonitrile were employed as mobile phases A and B, respectively. The mobile phase  
536 flow rate was 0.4 ml min<sup>-1</sup> and the injection volume was 1 µl. Liquid chromatography  
537 was coupled to a triple-quadrupole mass spectrometer (ABSciex Q-trap 5500). Other  
538 parameters were: curtain gas: 40 psi, collision gas: high, ion spray voltage (IS): 2.5  
539 keV, temperature: 550 °C, ion source gas: 1: 60 psi, ion source gas 2: 70 psi. Multiple  
540 reaction monitoring was used to determine the identity of the focal analyte. Analyst and  
541 Multiquant software (AB Sciex) were used to extract and analyze the data.

542

#### 543 *Amino acid profile-based distance calculation using supernatant data*

544 The similarity between closely related and distantly related donor amino acid profiles  
545 was measured by calculating the Euclidean distance. If the amino acid production of a  
546 closely related donor is given by  $CR = (cr_1, cr_2, \dots, cr_{20})$ , and the amino acid production  
547 of the distant related donor is given by  $DR = (dr_1, dr_2, \dots, dr_{20})$ , the Euclidean distance  
548 between recipient and donor is:

549

$$550 \quad ED(CR, DR) = \sqrt{(cr_1 - dr_1)^2 + (cr_2 - dr_2)^2 + \dots + (cr_{20} - dr_{20})^2}$$

551 Index numbers (1-20) refer to individual amino acids.

552

### 553 *Phylogenetic tree construction and distance calculation*

554 To cover a broad taxonomic diversity of donor strains, we chose 25 well-  
555 characterized species, belonging to four different phyla. The 16S rRNA gene  
556 sequences of 20 strains were retrieved from the NCBI GenBank and 5 strains from  
557 16S rRNA sequencing (see supplementary method). The phylogenetic tree of this  
558 marker gene was generated using the maximum likelihood method in MEGA X  
559 software (73). 16S rRNA gene locus sequences of all strains were converted to amino  
560 acid sequences and aligned with MUSCLE. Maximum-likelihood (ML) trees were  
561 constructed using the Kimura 2-parameter model, where rates and patterns among  
562 mutated sites were kept at uniform rates, yielding the best fit. Bootstrapping was  
563 carried out with 1,000 replicates. The phylogenetic tree was edited using the iTOL  
564 online tool (Table S7) (74). Pairwise phylogenetic distances between donor and  
565 receiver strains were extracted from a phylogenetic distance-based matrix. The  
566 resulting values quantify the evolutionary distance that separates the organisms.

567

### 568 *Reconstruction of metabolic networks*

569 Genome-scale metabolic networks for all organisms (Table S4) were reconstructed  
570 based on their genomic sequences using the GapSeq software (version v0.9,  
571 <https://github.com/jotech/gapseq>) (75). In brief, the reconstruction process is divided  
572 in two main steps. First, reactions and pathway predictions, and, second, gap-filling of  
573 the network to facilitate *in-silico* biomass production using flux balance analysis. For  
574 the reaction and pathway prediction step, all pathways from MetaCyc database (76)  
575 that are annotated for the taxonomic range of bacteria, were considered. Of each  
576 reaction within pathways, the protein sequences of the corresponding enzymes were  
577 retrieved from the SwissProt database (77) and aligned against the organism's  
578 genome sequence by the TBLASTN algorithm (78). An enzyme, and thus the  
579 corresponding reaction, was considered to be present in the organism's metabolic  
580 network, if the alignment's bitscore was  $\geq 200$  and the query coverage  $\geq 75\%$ .  
581 Moreover, reactions were considered to be existing, if more than 75% of the remaining  
582 reactions within the pathway were predicted to be present by the BLAST-searches or  
583 if more than 66% of the key enzymes, which are defined for each pathway by MetaCyc,  
584 were predicted to be part of the network by the blast searches. As reaction database  
585 for model construction, we used the ModelSEED database for metabolic modeling  
586 (79).

587 The second step (i.e., the gap filling algorithm of gapseq) solves several optimization  
588 problems by utilizing a minimum number of reactions from the ModelSEED database  
589 and adding them to the network, in order to facilitate growth in a given growth medium.  
590 Here, the chemical composition of the M9 medium (which is qualitatively identical to  
591 MMAB) with glucose as sole carbon source was assumed.

592

### 593 *Calculating the genome-based metabolic distance of organisms*

594 To estimate the pairwise metabolic distance between donor and recipient  
595 genotypes, the structure of their metabolic network was compared. For this, a flux  
596 balance analysis was performed on each individual metabolic network model.  
597 Subsequently, total flux was minimized to predict the flux distribution in M9-glucose  
598 medium (80). Pairwise distances of flux distributions between organisms were  
599 calculated as the Euclidean distance between the predicted flux vectors. Only  
600 reactions with a non-zero flux in at least one of the two organisms were included in the  
601 distance approximations.

602

### 603 *In-silico simulation of bacterial co-growth*

604 To further investigate the relationship between the metabolic distance between  
605 organisms and the likelihood for them to enter into a cross-feeding interaction, we  
606 extended our analysis to a larger number of bacterial organisms using *in-silico* co-  
607 growth simulations. For this, we reconstructed 818 bacterial metabolic network models  
608 as described above. The selected 818 organisms are the same as from the AGORA-  
609 collection, which represent common members of the human gut microbiota (81). For  
610 co-growth simulations, the models were merged in a pairwise manner as described  
611 previously (82). The predicted metabolic flux distributions of bacterial co-growth  
612 simulations were used to estimate the *metabolic exchange* between organisms. The  
613 metabolic exchange between two organisms was calculated as the sum of absolute  
614 predicted exchange rates (exchange fluxes) of metabolites. A logistic curve function of  
615 the form  $y(x) = a / (1 + e^{-b(x-c)})$  was fitted to the data using R (83).

616

### 617 *Statistical data analysis*

618 Normal distribution of data was evaluated by means of the Kolmogorov-Smirnov test  
619 and data was considered to be normally distributed when  $P > 0.05$ . Homogeneity of  
620 variance was determined using Levene's test and variances were considered  
621 homogenous if  $P > 0.05$ . Differences in the recipient growth in coculture versus  
622 monocultures were assessed with paired sample t-tests. P-values were corrected for  
623 multiple testing by applying the false discovery rate (FDR) procedure of Benjamini *et*  
624 *al.* (84, 85). Linear regressions were used to assess the growth support of recipients  
625 in cocultures as a function of different variables (i.e. amino acid profile distance,  
626 phylogenetic distances, metabolic distance). Spearman's rank correlation was used to  
627 assess the relationship between amino acid production and growth of recipient as  
628 maximum density when cultured with donor supernatants. The relationship between  
629 each proxy tested and recipient growth was depicted as a 2D plane and analyzed by



630 fitting a linear regression. Regression analyses was also used to disentangle the effect  
631 of more than one interacting predictor variable. In these cases, the phylogenetic signal  
632 or amino acid produced was controlled for the respective other predictor variable (e.g.  
633 metabolic distance or amino acid production profile distance) used to predict growth of  
634 recipient (Table S7).

635

### 636 **Acknowledgements**

637 We thank the entire Kost lab (past and present) for useful discussion as well as Marita  
638 Hermann and Antje Moehlmeyer for technical assistance. We are grateful to Stefan  
639 Walter and Saskia Schuback (CellNanOS, MS facility) for help with quantifying the exo-  
640 metabolome, Heiko Vogel and Domenica Schnabelrauch (Department of Entomology,  
641 MPI-CE) for help in 16s rRNA sequencing, Ákos T. Kovács, (Technical University of  
642 Denmark; Denmark) for sharing two *Bacillus subtilis* strains and Michael Hensel,  
643 (Department of Microbiology, University of Osnabrück; Germany) for providing *Serratia*  
644 *ficaria* strain. This work was funded by the German Research Foundation (SPP1617,  
645 KO 3909/2-1: CK, SG), (SFB 944, P19: CK), (KO 3909/4-1: CK), and the University of  
646 Osnabrück (LO, *EvoCell*: CK). CKa and SW acknowledge support by the German  
647 Research Foundation within the scope of the Excellence Cluster “Precision medicine  
648 in chronic inflammation” (EXC2167, sub-project RTF-VIII) and the Collaborative  
649 research center “Metaorganisms” (SFB1182, sub-project A1).

650

### 651 **Author contributions**

652 SG and CKo conceived the project. SG, SS, and CKo designed the research. SG  
653 performed all experiments. SG and LO analyzed the data. SG, LO, and CKo  
654 interpreted the data. SW calculated the genome-scale metabolic distance of tested  
655 strains and performed all *in-silico* analyses. SW and CKa carried out the gut  
656 microbiome *in-silico* data collection. GY isolated and phenotypically characterized the  
657 five environmentally-derived donor strains. SG and CKo wrote the manuscript, all  
658 authors revised the manuscript. CKo provided resources and acquired funding.

659

### 660 **Competing interests**

661 The authors declare no competing interests.

662

### 663 **References**

664

- 665 1. N. Fierer, R. B. Jackson, The diversity and biogeography of soil bacterial communities.  
666 *Proceedings of the National Academy of Sciences of the United States of America* **103**,  
667 626-631 (2006).
- 668 2. C. A. Lozupone, R. Knight, Global patterns in bacterial diversity. *Proceedings of the*  
669 *National Academy of Sciences* **104**, 11436-11440 (2007).
- 670 3. P. G. Falkowski, T. Fenchel, E. F. Delong, The microbial engines that drive earth's  
671 biogeochemical cycles. *Science* **320**, 1034-1039 (2008).

- 672 4. N. Fierer, Embracing the unknown: disentangling the complexities of the soil microbiome.  
673 *Nature Reviews Microbiology* **15**, 579-590 (2017).
- 674 5. R. Mendes *et al.*, Deciphering the rhizosphere microbiome for disease-suppressive  
675 bacteria. *Science* **332**, 1097-1100 (2011).
- 676 6. M. Saleem, J. Hu, A. Jousset, More than the sum of its parts: microbiome biodiversity as  
677 a driver of plant growth and soil health. *Annual Review of Ecology, Evolution, and*  
678 *Systematics* **50**, 145-168 (2019).
- 679 7. C. W. Russell *et al.*, Matching the supply of bacterial nutrients to the nutritional demand of  
680 the animal host. *Proceedings of the Royal Society B: Biological Sciences* **281**, 20141163  
681 (2014).
- 682 8. W. K. Kwong *et al.*, Dynamic microbiome evolution in social bees. *Science Advances* **3**,  
683 e1600513 (2017).
- 684 9. A. L. Kau, P. P. Ahern, N. W. Griffin, A. L. Goodman, J. I. Gordon, Human nutrition, the  
685 gut microbiome and the immune system. *Nature* **474**, 327-336 (2011).
- 686 10. S. V. Lynch, O. Pedersen, The human intestinal microbiome in health and disease. *New*  
687 *England Journal of Medicine* **375**, 2369-2379 (2016).
- 688 11. G. E. Leventhal *et al.*, Strain-level diversity drives alternative community types in  
689 millimetre-scale granular biofilms. *Nature Microbiology* **3**, 1295-1303 (2018).
- 690 12. D. W. Rivett, T. Bell, Abundance determines the functional role of bacterial phylotypes in  
691 complex communities. *Nature Microbiology* **3**, 767-772 (2018).
- 692 13. S. Giri, S. Shitut, C. Kost, Harnessing ecological and evolutionary principles to guide the  
693 design of microbial production consortia. *Current Opinion in Biotechnology* **62**, 228-238  
694 (2020).
- 695 14. W. Kong, D. R. Meldgin, J. J. Collins, T. Lu, Designing microbial consortia with defined  
696 social interactions. *Nature Chemical Biology* **14**, 821-829 (2018).
- 697 15. C. Rezzoagli, E. T. Granato, R. Kümmerli, Harnessing bacterial interactions to manage  
698 infections: a review on the opportunistic pathogen *Pseudomonas aeruginosa* as a case  
699 example. *Journal of Medical Microbiology* **69**, 147-161 (2020).
- 700 16. G. D'Souza *et al.*, Ecology and evolution of metabolic cross-feeding interactions in  
701 bacteria. *Natural Product Reports* **35**, 455-488 (2018).
- 702 17. K. Zengler, L. S. Zaramela, The social network of microorganisms — how auxotrophies  
703 shape complex communities. *Nature Reviews Microbiology* **16**, 383-390 (2018).
- 704 18. O. X. Cordero, M. S. Datta, Microbial interactions and community assembly at  
705 microscales. *Current Opinion in Microbiology* **31**, 227-234 (2016).
- 706 19. T. N. Enke *et al.*, Modular assembly of polysaccharide-degrading marine microbial  
707 communities. *Current Biology* **29**, 1528-1535.e1526 (2019).
- 708 20. S. Sieuwerts *et al.*, Mixed-culture transcriptome analysis reveals the molecular basis of  
709 mixed-culture growth in *Streptococcus thermophilus* and *Lactobacillus bulgaricus*. *Applied*  
710 *and Environmental Microbiology* **76**, 7775-7784 (2010).
- 711 21. O. Ponomarova *et al.*, Yeast creates a niche for symbiotic lactic acid bacteria through  
712 nitrogen overflow. *Cell Systems* **5**, 345-357.e346 (2017).
- 713 22. M. T. Croft, A. D. Lawrence, E. Raux-Deery, M. J. Warren, A. G. Smith, Algae acquire  
714 vitamin B12 through a symbiotic relationship with bacteria. *Nature* **438**, 90-93 (2005).
- 715 23. O. M. Sokolovskaya, A. N. Shelton, M. E. Taga, Sharing vitamins: Cobamides unveil  
716 microbial interactions. *Science* **369**, eaba0165 (2020).
- 717 24. A. Loera-Muro *et al.*, Auxotrophic *Actinobacillus pleurpneumoniae* grows in multispecies  
718 biofilms without the need for nicotinamide-adenine dinucleotide (NAD) supplementation.  
719 *BMC Microbiology* **16**, 128 (2016).

- 720 25. S. Rakoff-Nahoum, Michael J. Coyne, Laurie E. Comstock, An ecological network of  
721 polysaccharide utilization among human intestinal symbionts. *Current Biology* **24**, 40-49  
722 (2014).
- 723 26. N. Paczia *et al.*, Extensive exometabolome analysis reveals extended overflow  
724 metabolism in various microorganisms. *Microb. Cell. Fact.* **11**, 122 (2012).
- 725 27. A. E. Douglas, The microbial exometabolome: ecological resource and architect of  
726 microbial communities. *Philosophical Transactions of the Royal Society B: Biological*  
727 *Sciences* **375**, 20190250 (2020).
- 728 28. K. Campbell, L. Herrera-Dominguez, C. Correia-Melo, A. Zelezniak, M. Ralsler,  
729 Biochemical principles enabling metabolic cooperativity and phenotypic heterogeneity at  
730 the single cell level. *Current Opinion in Systems Biology* **8**, 97-108 (2018).
- 731 29. B. Schink, Synergistic interactions in the microbial world. *Antonie van Leeuwenhoek* **81**,  
732 257-261 (2002).
- 733 30. J. J. Morris, Black Queen evolution: the role of leakiness in structuring microbial  
734 communities. *Trends in Genetics* **31**, 475-482 (2015).
- 735 31. O. X. Cordero, L.-A. Ventouras, E. F. DeLong, M. F. Polz, Public good dynamics drive  
736 evolution of iron acquisition strategies in natural bacterioplankton populations.  
737 *Proceedings of the National Academy of Sciences* **109**, 20059-20064 (2012).
- 738 32. M. Schuster, D. J. Sexton, S. P. Diggle, E. P. Greenberg, Acyl-homoserine lactone quorum  
739 sensing: from evolution to application. *Annual Review of Microbiology* **67**, 43-63 (2013).
- 740 33. A. Zelezniak *et al.*, Metabolic dependencies drive species co-occurrence in diverse  
741 microbial communities. *Proceedings of the National Academy of Sciences* **112**, 6449-6454  
742 (2015).
- 743 34. S. Giri, S. Waschina, C. Kaleta, C. Kost, Defining division of labor in microbial  
744 communities. *Journal of Molecular Biology* **23**, 4712-4731 (2019).
- 745 35. S. J. Giovannoni, J. Cameron Thrash, B. Temperton, Implications of streamlining theory  
746 for microbial ecology. *The ISME Journal* **8**, 1553-1565 (2014).
- 747 36. R. Baran *et al.*, Exometabolite niche partitioning among sympatric soil bacteria. *Nature*  
748 *Communications* **6**, 8289 (2015).
- 749 37. E. Butaite, M. Baumgartner, S. Wyder, R. Kummerli, Siderophore cheating and cheating  
750 resistance shape competition for iron in soil and freshwater *Pseudomonas* communities.  
751 *Nat Commun* **8**, 414 (2017).
- 752 38. S. L. Garcia *et al.*, Auxotrophy and intrapopulation complementary in the 'interactome' of  
753 a cultivated freshwater model community. *Molecular Ecology* **24**, 4449-4459 (2015).
- 754 39. S. J. Macdonald, G. G. Lin, C. W. Russell, G. H. Thomas, A. E. Douglas, The central role  
755 of the host cell in symbiotic nitrogen metabolism. *Proceedings of the Royal Society B:*  
756 *Biological Sciences* **279**, 2965-2973 (2012).
- 757 40. A. Narwani, M. A. Alexandrou, T. H. Oakley, I. T. Carroll, B. J. Cardinale, Experimental  
758 evidence that evolutionary relatedness does not affect the ecological mechanisms of  
759 coexistence in freshwater green algae. *Ecology Letters* **16**, 1373-1381 (2013).
- 760 41. J. Russel, H. L. Roder, J. S. Madsen, M. Burmolle, S. J. Sorensen, Antagonism correlates  
761 with metabolic similarity in diverse bacteria. *Proc Natl Acad Sci U S A* **114**, 10684-10688  
762 (2017).
- 763 42. C. Xenophontos, M. Taubert, W. S. Harpole, K. Küsel, Phylogenetic and functional  
764 diversity have contrasting effects on the ecological functioning of bacterial communities.  
765 *bioRxiv* 10.1101/839696, 839696 (2019).
- 766 43. D. Machado *et al.*, Polarization of microbial communities between competitive and  
767 cooperative metabolism. *bioRxiv* 10.1101/2020.01.28.922583, 2020.2001.2028.922583  
768 (2020).

- 769 44. D. Wall, Kin Recognition in Bacteria. *Annu Rev Microbiol* **70**, 143-160 (2016).
- 770 45. M. Wang, A. L. Schaefer, A. A. Dandekar, E. P. Greenberg, Quorum sensing and policing  
771 of *Pseudomonas aeruginosa* social cheaters. *Proceedings of the National Academy of*  
772 *Sciences* **112**, 2187-2191 (2015).
- 773 46. S. Smukalla *et al.*, FLO1 is a variable green beard gene that drives biofilm-like cooperation  
774 in budding yeast. *Cell* **135**, 726-737 (2008).
- 775 47. P. Stefanic, B. Kraigher, N. A. Lyons, R. Kolter, I. Mandic-Mulec, Kin discrimination  
776 between sympatric *Bacillus subtilis* isolates. *Proceedings of the National Academy of*  
777 *Sciences* **112**, 14042-14047 (2015).
- 778 48. S. Pande *et al.*, Metabolic cross-feeding via intercellular nanotubes among bacteria.  
779 *Nature Communications* **6**, 6238 (2015).
- 780 49. S. Shitut, T. Ahsendorf, S. Pande, M. Egbert, C. Kost, Nanotube-mediated cross-feeding  
781 couples the metabolism of interacting bacterial cells. *Environ Microbiol* **21**, 1306-1320  
782 (2019).
- 783 50. S. Bernhardsson, P. Gerlee, L. Lizana, Structural correlations in bacterial metabolic  
784 networks. *BMC Evolutionary Biology* **11**, 20 (2011).
- 785 51. E. R. Hester, M. S. M. Jetten, C. U. Welte, S. Lücker, Metabolic overlap in environmentally  
786 diverse microbial communities. *Frontiers in Genetics* **10** (2019).
- 787 52. S. Waschina, G. D'Souza, C. Kost, C. Kaleta, Metabolic network architecture and carbon  
788 source determine metabolite production costs. *The FEBS Journal* **283**, 2149-2163 (2016).
- 789 53. H. Akashi, T. Gojobori, Metabolic efficiency and amino acid composition in the proteomes  
790 of *Escherichia coli* and *Bacillus subtilis*. *Proceedings of the National Academy of Sciences*  
791 **99**, 3695-3700 (2002).
- 792 54. N. P. Zakataeva, V. V. Aleshin, I. L. Tokmakova, P. V. Troshin, V. A. Livshits, The novel  
793 transmembrane *Escherichia coli* proteins involved in the amino acid efflux. *FEBS Letters*  
794 **452**, 228-232 (1999).
- 795 55. V. Doroshenko *et al.*, YddG from *Escherichia coli* promotes export of aromatic amino  
796 acids. *FEMS Microbiology Letters* **275**, 312-318 (2007).
- 797 56. L. G. Airich *et al.*, Membrane Topology Analysis of the *Escherichia coli* aromatic amino  
798 acid efflux protein YddG. *Journal of Molecular Microbiology and Biotechnology* **19**, 189-  
799 197 (2010).
- 800 57. B. E. L. Morris, R. Henneberger, H. Huber, C. Moissl-Eichinger, Microbial syntrophy:  
801 interaction for the common good. *FEMS Microbiology Reviews* **37**, 384-406 (2013).
- 802 58. O. Ponomarova, K. R. Patil, Metabolic interactions in microbial communities: untangling  
803 the Gordian knot. *Current Opinion in Microbiology* **27**, 37-44 (2015).
- 804 59. J. Swire, Selection on synthesis cost affects interprotein amino acid usage in all three  
805 domains of life. *Journal of Molecular Evolution* **64**, 558-571 (2007).
- 806 60. J. L. Barker *et al.*, Synthesizing perspectives on the evolution of cooperation within and  
807 between species. *Evolution* **71**, 814-825 (2017).
- 808 61. S. Westhoff, A. Kloosterman, S. F. A. van Hoesel, G. P. van Wezel, D. E. Rozen,  
809 Competition sensing alters antibiotic production in *Streptomyces*. *bioRxiv*  
810 10.1101/2020.01.24.918557, 2020.2001.2024.918557 (2020).
- 811 62. J. L. Bronstein, Our Current Understanding of Mutualism. *The Quarterly Review of Biology*  
812 **69**, 31-51 (1994).
- 813 63. E. T. Kiers, R. A. Rousseau, S. A. West, R. F. Denison, Host sanctions and the legume-  
814 rhizobium mutualism. *Nature* **425**, 78-81 (2003).
- 815 64. M. McFall-Ngai, Hawaiian bobtail squid. *Current Biology* **18**, R1043-R1044 (2008).
- 816 65. H. Ogata *et al.*, KEGG: Kyoto Encyclopedia of Genes and Genomes. *Nucleic Acids*  
817 *Research* **27**, 29-34 (1999).

- 818 66. I. M. Keseler *et al.*, EcoCyc: a comprehensive database of *Escherichia coli* biology.  
819 *Nucleic Acids Research* **39**, D583-D590 (2010).
- 820 67. T. Baba *et al.*, Construction of *Escherichia coli* K-12 in-frame, single-gene knockout  
821 mutants: the Keio collection. *Molecular Systems Biology* **2**, 2006.0008 (2006).
- 822 68. L. C. Thomason, N. Costantino, D. L. Court, *E. coli* genome manipulation by P1  
823 transduction. *Current Protocols in Molecular Biology* **79**, 1.17.11-11.17.18 (2007).
- 824 69. A. R. Joyce *et al.*, Experimental and computational assessment of conditionally essential  
825 genes in *Escherichia coli*. *Journal of Bacteriology* **188**, 8259-8271 (2006).
- 826 70. M. Vanstockem, K. Michiels, J. Vanderleyden, A. P. Van Gool, Transposon Mutagenesis  
827 of *Azospirillum brasilense* and *Azospirillum lipoferum*: Physical analysis of Tn5 and Tn5-  
828 Mob insertion mutants. *Applied and Environmental Microbiology* **53**, 410-415 (1987).
- 829 71. Y. Tapuhi, D. E. Schmidt, W. Lindner, B. L. Karger, Dansylation of amino acids for high-  
830 performance liquid chromatography analysis. *Analytical Biochemistry* **115**, 123-129  
831 (1981).
- 832 72. T. Takeuchi, "1.2.5. - HPLC of amino acids as dansyl and dabsyl derivatives" in Journal  
833 of Chromatography Library, I. Molnár-Perl, Ed. (Elsevier, 2005), vol. 70, pp. 229-241.
- 834 73. S. Kumar, G. Stecher, M. Li, C. Knyaz, K. Tamura, MEGA X: Molecular Evolutionary  
835 Genetics Analysis across Computing Platforms. *Molecular Biology and Evolution* **35**,  
836 1547-1549 (2018).
- 837 74. I. Letunic, P. Bork, Interactive Tree Of Life (iTOL): an online tool for phylogenetic tree  
838 display and annotation. *Bioinformatics* **23**, 127-128 (2006).
- 839 75. J. Zimmermann, C. Kaleta, S. Waschina, gapseq: Informed prediction of bacterial  
840 metabolic pathways and reconstruction of accurate metabolic models. *bioRxiv*  
841 10.1101/2020.03.20.000737, 2020.2003.2020.000737 (2020).
- 842 76. P. D. Karp, M. Riley, S. M. Paley, A. Pellegrini-Toole, The metaCyc database. *Nucleic*  
843 *Acids Research* **30**, 59-61 (2002).
- 844 77. E. Boutet, D. Lieberherr, M. Tognolli, M. Schneider, A. Bairoch, "UniProtKB/Swiss-Prot" in  
845 plant bioinformatics: Methods and protocols, D. Edwards, Ed. (Humana Press, Totowa,  
846 NJ, 2007), 10.1007/978-1-59745-535-0\_4, pp. 89-112.
- 847 78. J. Ye, S. McGinnis, T. L. Madden, BLAST: improvements for better sequence analysis.  
848 *Nucleic Acids Research* **34**, W6-W9 (2006).
- 849 79. S. Devoid *et al.*, "Automated genome annotation and metabolic model reconstruction in  
850 the SEED and Model SEED" in systems metabolic engineering: Methods and Protocols,  
851 H. S. Alper, Ed. (Humana Press, Totowa, NJ, 2013), 10.1007/978-1-62703-299-5\_2, pp.  
852 17-45.
- 853 80. H.-G. Holzhütter, The principle of flux minimization and its application to estimate  
854 stationary fluxes in metabolic networks. *European Journal of Biochemistry* **271**, 2905-2922  
855 (2004).
- 856 81. S. Magnúsdóttir *et al.*, Generation of genome-scale metabolic reconstructions for 773  
857 members of the human gut microbiota. *Nature Biotechnology* **35**, 81-89 (2017).
- 858 82. K. Aden *et al.*, Metabolic functions of gut microbes associate with efficacy of tumor  
859 necrosis factor antagonists in patients with inflammatory bowel diseases.  
860 *Gastroenterology* **157**, 1279-1292.e1211 (2019).
- 861 83. R. C. Team (2013) R: A language and environment for statistical computing. (Vienna,  
862 Austria).
- 863 84. Y. Benjamini, Y. Hochberg, Controlling the False Discovery Rate: a practical and powerful  
864 approach to multiple testing. *Journal of the Royal Statistical Society: Series B*  
865 (*Methodological*) **57**, 289-300 (1995).

866 85. Y. Benjamini, A. M. Krieger, D. Yekutieli, Adaptive linear step-up procedures that control  
867 the false discovery rate. *Biometrika* **93**, 491-507 (2006).

868